

# Translocation of XRCC1 and DNA ligase III $\alpha$ from centrosomes to chromosomes in response to DNA damage in mitotic human cells

Satoshi Okano<sup>1,2</sup>, Li Lan<sup>1</sup>, Alan E. Tomkinson<sup>3</sup> and Akira Yasui<sup>1,\*</sup>

<sup>1</sup>Department of Molecular Genetics, Institute of Development, Aging and Cancer, Tohoku University, 980-8575 Sendai, Japan, <sup>2</sup>Research Laboratory for Molecular Genetics, Yamagata University, 990-9585 Yamagata, Japan and <sup>3</sup>Radiation Research Laboratory, Department of Radiation Oncology and Greenebaum Cancer Center, University of Maryland School of Medicine, 655 West Baltimore Street, Baltimore, MD 21201-1509, USA

Received December 22, 2004; Accepted December 22, 2004

## ABSTRACT

DNA single-strand breaks (SSBs) are the most frequent lesions caused by oxidative DNA damage. They disrupt DNA replication, give rise to double-strand breaks and lead to cell death and genomic instability. It has been shown that the XRCC1 protein plays a key role in SSBs repair. We have recently shown in living human cells that XRCC1 accumulates at SSBs in a fully poly(ADP-ribose) (PAR) synthesis-dependent manner and that the accumulation of XRCC1 at SSBs is essential for further repair processes. Here, we show that XRCC1 and its partner protein, DNA ligase III $\alpha$ , localize at the centrosomes and their vicinity in metaphase cells and disappear during anaphase. Although the function of these proteins in centrosomes during metaphase is unknown, this centrosomal localization is PAR-dependent, because neither of the proteins is observed in the centrosomes in the presence of PAR polymerase inhibitors. On treatment of metaphase cells with H<sub>2</sub>O<sub>2</sub>, XRCC1 and DNA ligase III $\alpha$  translocate immediately from the centrosomes to mitotic chromosomes. These results show for the first time that the repair of SSBs is present in the early mitotic chromosomes and that there is a dynamic response of XRCC1 and DNA ligase III $\alpha$  to SSBs, in which these proteins are recruited from the centrosomes, where metaphase-dependent activation of PAR polymerase occurs, to mitotic chromosomes, by SSBs-dependent activation of PAR polymerase.

## INTRODUCTION

DNA single-strand breaks (SSBs) are generated directly by the action of DNA-damaging agents, such as ionizing radiation and active oxygen species. In addition, they arise as reaction intermediates during lagging strand DNA synthesis and DNA excision repair. There is compelling evidence that the DNA repair protein XRCC1 plays a critical role in the repair of SSBs [reviewed in (1)]. Notably, XRCC1 mutant cells exhibit an elevated frequency of spontaneous chromosomal aberrations and deletions (2), and inactivation of the mouse *Xrcc1* gene by gene targeting results in embryonic lethality (3), suggesting the importance of XRCC1-dependent repair in maintaining genome stability.

Although XRCC1 protein has no known catalytic activity, it does interact with many different protein partners, including OGG1 (4), PARP-1 (5,6,7), PARP-2 (7), DNA polymerase  $\beta$  (8,9), AP endonuclease (10), polynucleotide kinase (11) and DNA ligase III $\alpha$  (LIGIII $\alpha$ ) (12,13). These multiple interactions suggest that XRCC1 co-ordinates the repair of SSBs by acting as a scaffolding factor upon which the other SSB repair proteins assemble. The interaction between XRCC1 and LIGIII $\alpha$  is constitutive and stabilizes LIGIII $\alpha$  (14). Interestingly, studies, in which the LIGIII $\alpha$ -interacting BRCT domain of XRCC1 was inactivated, revealed that XRCC1 repair functions are LIGIII $\alpha$ -dependent in G1 phase cells and non-cycling cells but are LIGIII $\alpha$ -independent in S phase cells (15). These results suggest that the XRCC1/LIGIII $\alpha$  complex participates in SSBs repair and the repair of base lesions by the short patch sub-pathway of BER, whereas XRCC1 functions in certain S phase-specific repair events that are not well understood.

PARP-1 is the first member of a growing family of enzymes that synthesize poly(ADP-ribose) (PAR). PARP-1

\*To whom correspondence should be addressed. Tel: +81 22 717 8465; Fax: +81 22 717 8470; Email: ayasui@idac.tohoku.ac.jp

The online version of this article has been published under an open access model. Users are entitled to use, reproduce, disseminate, or display the open access version of this article for non-commercial purposes provided that: the original authorship is properly and fully attributed; the Journal and Oxford University Press are attributed as the original place of publication with the correct citation details given; if an article is subsequently reproduced or disseminated not in its entirety but only in part or as a derivative work this must be clearly indicated. For commercial re-use permissions, please contact journals.permissions@oupjournals.org.

is an abundant nuclear protein that binds avidly to DNA strand breaks, in particular DNA SSBs via two tandem arrayed N-terminal zinc fingers. The binding to SSBs activates the polymerase activity of PARP-1, resulting in the poly(ADP-ribosylation) of PARP-1 itself and other proteins. Although the exact role of PARP-1 in DNA repair remains the subject of conflicting reports, the spontaneous genetic instability and hypersensitivity to DNA-damaging agents of *parp-1* mutant cells provides compelling evidence that PARP-1 plays an important role in maintaining genomic integrity [reviewed in (16,17)]. Both XRCC1 (5,6,7) and LIGIII (18) preferentially bind to poly(ADP-ribosylated) PARP-1, suggesting that auto-modified PARP-1 molecules in the vicinity of SSBs may serve as the signal for the recruitment of SSBs repair proteins. In support of this idea, it has been shown that local ultraviolet (UV) irradiation of human nucleotide excision repair-deficient XPA cells expressing UV damage endonuclease (UVDE), which generates SSBs at UV-irradiated restricted regions in nucleus (19) or local laser irradiation (20), resulted in massive synthesis of PAR only within the irradiated regions. Moreover, it was shown that the accumulation of XRCC1 at SSBs is dependent upon PAR synthesis (19,20), and accumulation of polymerase  $\beta$  as well as proliferating cellular nuclear antigen (PCNA) at SSBs is dependent on the presence of XRCC1 (20). Thus, the accumulation of XRCC1 at SSBs is essential for both polymerase  $\beta$ -dependent short-patch and PCNA-dependent long-patch repair pathways.

Recently, it has been shown that several members of the PARP family, PARP-1 (21,22), PARP-3 (23), tankyrase (24) and PAR glycohydrolase (25), which degrades PAR polymers, localize to the centrosome in mitotic cells. This prompted us to examine whether XRCC1 and LIGIII $\alpha$  exhibit similar behavior. By using immunofluorescence and confocal microscopy, we show that both XRCC1 and LIGIII $\alpha$  are mainly localized within centrosomes during mitosis and that this sub-nuclear localization is dependent upon PAR synthesis. In response to DNA damage, both XRCC1 and LIGIII $\alpha$  translocate from the centrosomes region to the chromosomes providing the first evidence for the repair of SSBs in mitotic chromosomes.

## MATERIALS AND METHODS

### Cell lines and culture conditions

HeLa, XPA-UVDE and XPA-Vector cells (26) were grown in Eagle's minimal essential medium (Nissui) supplemented with 10% fetal bovine serum.

### DNA transfection

DNA constructs were made according to the standard procedures (27). Briefly, the cDNA of full-length human LIGIII $\alpha$  was amplified by using PCR with 5' and 3' primers containing Sall and EcoRV sites, respectively. The amplified DNA fragments were subcloned into the Sall and SmaI sites of pEGFP-C1 (Clontech). A CHPL-GFP plasmid (obtained from Dr Phanglang Chen) contains a CMV promoter and drives the expression of an in-frame N-terminal green fluorescent protein (GFP) protein. The cDNA of full-length LIGIII $\beta$  was subcloned into the NotI site of the modified CHPL-GFP plasmid. The plasmid expressing full-length XRCC1 tagged with GFP is described previously (20).

The DNA constructs were verified by sequencing. These plasmids were introduced into cells using Fugene 6 (Roche) according to the manufacturer's protocol.

### Immunofluorescence microscopy

For immunolabeling, asynchronous HeLa cells were grown for 2 days in glass bottom culture dishes. To examine the effect of inhibitors of PARP, the cells were incubated for 1 h in medium supplemented with 3-aminobenzamide (3-AB) (8 mM; Sigma), fixed with methanol:acetone (1:1) for 10 min at  $-20^{\circ}\text{C}$ , then dried. In some cases, the cells were fixed by incubation in 4% formaldehyde in phosphate-buffered saline (PBS) for 10 min at RT, then permeabilized in 0.2% Triton X-100 in PBS for 2 min at RT. Local UV-irradiation, in which XPA-UVDE or XPA-Vector cells were irradiated through tiny pores in polycarbonate membrane filter, was performed essentially as described previously (19). XPA-UVDE or XPA-Vector cells were incubated for 1 h in medium supplemented with or without 1,5-dihydroxyisoquinoline (DIQ) (100  $\mu\text{M}$ ; Sigma) before irradiation, and washed twice with Hanks' solution (Nissui) with or without DIQ. Then, the cells were irradiated with UV (20  $\text{J}/\text{m}^2$ ). After local UV-irradiation, the cells were incubated in medium with or without DIQ at  $37^{\circ}\text{C}$  for 2 min, and then fixed as described above. Fixed cells were rinsed once with TNT buffer (0.1 M Tris-HCl, 0.15 M NaCl, 0.05% Tween 20, pH 7.5) and then incubated in TNB buffer [TNT buffer containing blocking reagent (NEN)] at  $30^{\circ}\text{C}$  for 30 min. After incubation with anti-XRCC1 antibody (ab144, Abcam) at 1:150 dilution in TNB buffer at  $30^{\circ}\text{C}$  for 1 h, the cells were washed three times with TNT buffer prior to incubation with Alexa Fluor 594 goat anti-rabbit immunoglobulin G (IgG) conjugate (Molecular Probes) at 1:400 dilution in TNB buffer for 1 h. The cells were washed with TNT buffer and then incubated with anti- $\gamma$ -tubulin (1:200 dilution, GTU-88; Sigma), anti-PAR (1:200 dilution; Trevigen) or anti-DNA LIGIII (1:50 dilution; GeneTex 1F3 or 4C11) in TNB buffer for 1 h. After washing with TNT buffer, the cells were incubated with Alexa Fluor 488 goat anti-mouse IgG conjugate (Molecular Probes) at 1:400 dilution in TNB buffer for 1 h. The cells were washed and then incubated with TOPRO-3 (2  $\mu\text{g}/\text{ml}$ , Molecular Probes) and RNaseA (100  $\mu\text{g}/\text{ml}$ ; Sigma) in PBS at  $37^{\circ}\text{C}$  for 15 min. After washing, the cell samples were mounted in drops of PermaFluor (Immunon), and cover-slips were added. Confocal imaging was performed using an Olympus FV-500 confocal laser system connected to an Olympus microscope (IX81) with a 60 $\times$  oil immersion objective lens (PlanApo).

## RESULTS AND DISCUSSION

### DNA ligase III $\alpha$ is recruited to SSB in response to the synthesis of PAR

Previously, using local UV-irradiation of human nucleotide excision repair-deficient XPA cells expressing UVDE, we had shown that PAR synthesis occurred only within the UV-irradiated regions and that the recruitment of XRCC1 to these regions was dependent upon PAR synthesis (19). Since there is evidence that XRCC1 functions independently of LIGIII $\alpha$  under certain circumstances (15,28), we asked whether LIGIII $\alpha$  was also recruited to the sites of SSBs

induced by the action of UVDE in XPA cells after local UV-irradiation. As shown previously (19), XRCC1 accumulated at the irradiated spots 2 min after irradiation (Figure 1, column b, upper panel). LIGIII $\alpha$  was also recruited to the same sites of DNA damage (Figure 1, column b, middle and bottom panels). As was observed with XRCC1, the recruitment of LIGIII $\alpha$  to the DNA damage sites was dependent upon the expression of UVDE (Figure 1, column e) and was prevented by DIQ (100  $\mu$ M), an inhibitor of PARP (Figure 1 column c). To confirm that the DNA damage-dependent sub-nuclear location of LIGIII $\alpha$  was not an artifact of the immunocytochemistry, we transiently expressed a GFP-tagged version of LIGIII $\alpha$  in XPA-UVDE cells. In accord with the results described above, GFP-LIGIII $\alpha$  was observed in the nucleolus as well as in the nucleoplasm of undamaged cells (Figure 2, column a) and was recruited to the sites of DNA damage induced by irradiation through a membrane filter (Figure 2, column b). Together, these results demonstrate that LIGIII $\alpha$ , like its protein partner XRCC1, translocates to the sites of SSBs and that this DNA damage-induced sub-nuclear relocation is dependent upon PAR synthesis. This is consistent with our recent results using local laser irradiation (20). To examine whether the recruitment of LIGIII $\alpha$  to SSBs is dependent upon XRCC1 and not on PARP-1, we transiently expressed a GFP-tagged version of DNA ligase III $\beta$  (LIGIII $\beta$ ), which is normally only expressed in meiotic cells (29). Importantly, LIGIII $\beta$  interacts with poly(ADP-ribosylated) PARP-1 (18) but does not bind to XRCC1. In undamaged cells, LIGIII $\beta$  was present in the nucleolus as well as in the nucleoplasm (Figure 2 column d), but, unlike LIGIII $\alpha$ , LIGIII $\beta$  was not recruited to the sites of DNA damage (Figure 2, column e).

By a more sensitive assay using UVA laser irradiation and GFP-tagged LIGIII $\alpha$ , we found a weak accumulation of LIGIII $\alpha$  at SSBs in XRCC1-deficient cells (L. Lan and A. Yasui, unpublished results), which may be explained by direct interaction between PARP-1 and LIGIII $\alpha$ . Thus, although LIGIII $\alpha$  binds to poly(ADP-ribosylated) PARP-1 *in vitro*, the *in vivo* recruitment of LIGIII $\alpha$  to SSBs is mainly dependent upon its C-terminal BRCT domain, which is required for the interaction with XRCC1 (29,30).

### XRCC1 and LIGIII $\alpha$ localize to the centrosomes

When exponentially growing HeLa cells were stained with an XRCC1 antibody, a unique staining pattern that appeared to correspond to the centrosomes was observed in both interphase and mitotic cells. To confirm the co-localization of XRCC1 with the centrosomes, we conducted a series of double-staining experiments using antibodies specific for XRCC1 and  $\gamma$ -tubulin, which is a component of pericentriolar matrix of the centrosome (31). As reported previously (19), the majority of XRCC1 in interphase cells is in the nucleoli, but a small fraction co-localized precisely with the two closely spaced dots of  $\gamma$ -tubulin located near the nuclear envelope (Figure 3A), which correspond to the duplicated centrosomes. The co-localization of XRCC1 with unduplicated centrosomes in interphase cells was also observed (data not shown). As described later, the presence of PAR in the centrosomes is crucial for the centrosomal localization of XRCC1. Detection of XRCC1 in the fraction of the centrosomes by antibodies failed, possibly because the amount of PAR polymers present in the centrosomes is limited partially due to the presence of

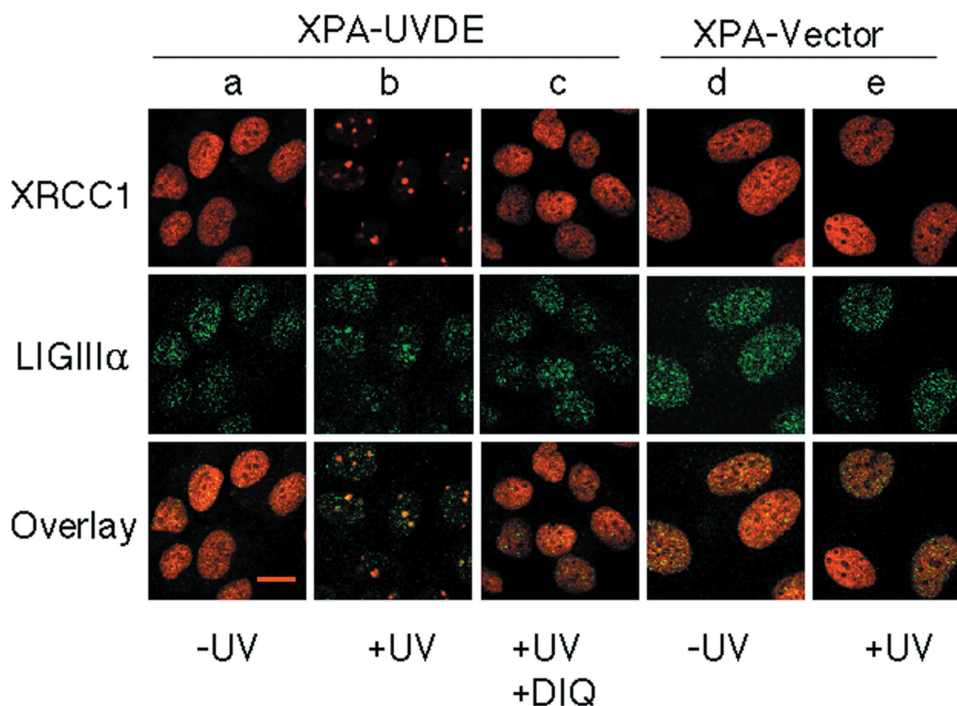


**Figure 1.** Accumulation of XRCC1 and LIGIII $\alpha$  at SSBs after local UV-irradiation in XPA-UVDE cells. Co-localization of XRCC1 with LIGIII $\alpha$  was identified by double immunolabeling. Two minutes after local UV-irradiation (20 J/m<sup>2</sup>) cells were fixed with paraformaldehyde and co-stained with anti-XRCC1 antibody (red, upper row) and anti-LIGIII $\alpha$  antibody (green, middle row); the column c is for XPA-UVDE cells treated with DIQ, an inhibitor of PARP, before UV-irradiation. Co-localization of XRCC1 with LIGIII $\alpha$  appears yellow in overlay (bottom row).

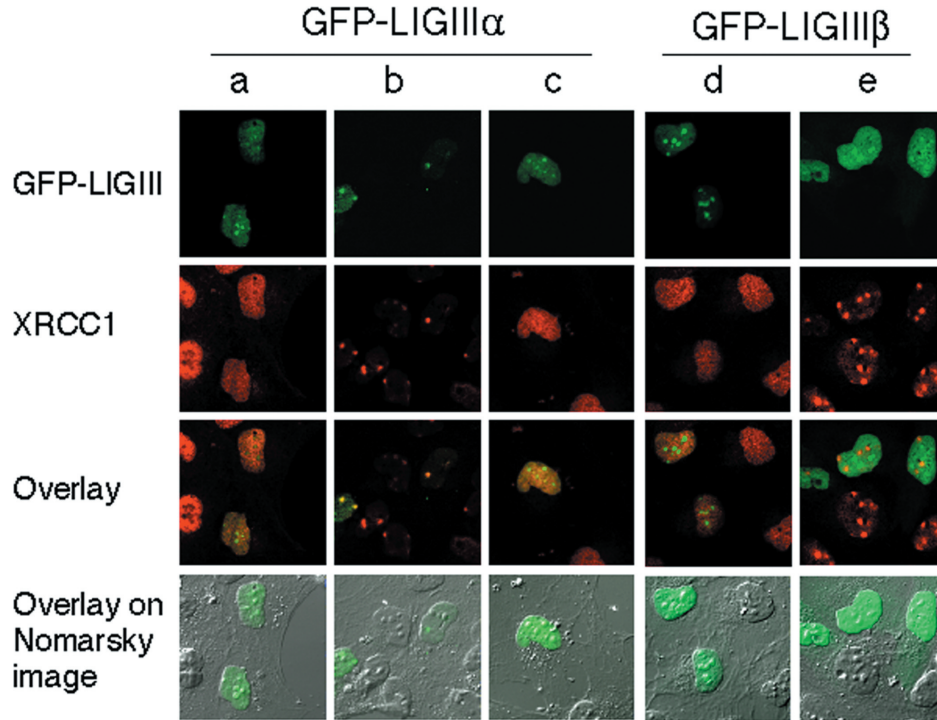


**Figure 2.** *In situ* visualization of GFP-DNA Ligase III $\alpha$ , GFP-DNA Ligase III $\beta$  and XRCC1 before and after local UV-irradiation. GFP-DNA Ligase III $\alpha$  (GFP-LIGIII $\alpha$ ) and GFP-DNA Ligase III $\beta$  (GFP-LIGIII $\beta$ ) were transiently expressed in XPA-UVDE cells before UV-irradiation (20 J/m<sup>2</sup>). The fluorescence images of the cells stained with anti-XRCC1 (red, second upper row) and the images of GFP (green, uppermost row) are shown. Co-localization appears yellow (third row). GFP-tagged proteins were visualized 2 min after local UV-irradiation (20 J/m<sup>2</sup>). Column c is for DIQ treated cells. The fluorescent images of GFP were superimposed onto the Nomarsky images in the bottom row.

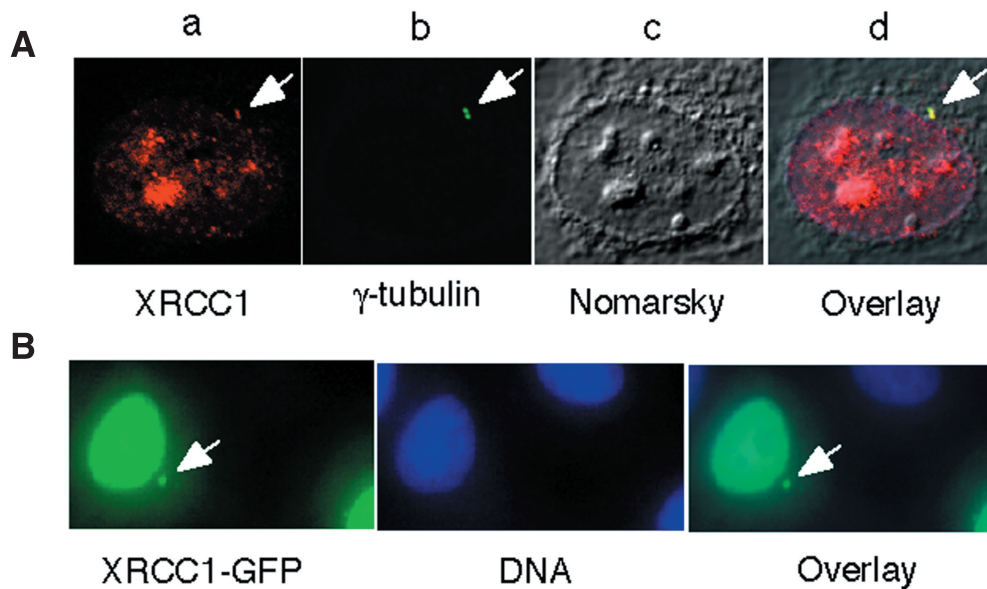


**Figure 3.** XRCC1 in centrosomes of HeLa cells during interphase. (A) Fluorescent micrographs of HeLa cells in interphase obtained by double immunolabeling for  $\gamma$ -tubulin and XRCC1. Cells were fixed with methanol:acetone and co-stained with anti-XRCC1 antibody (a), and anti- $\gamma$ -tubulin antibody (b). XRCC1 and  $\gamma$ -tubulin appear red and green, respectively. The corresponding Nomarsky image is shown in (c). Co-localization of both XRCC1 and  $\gamma$ -tubulin appears yellow in overlay (d). (B) Fluorescent micrographs of HeLa cells in interphase expressing XRCC1-GFP. The cells were fixed with paraformaldehyde. DNA was stained with TOPRO-3 (middle panel) and superimposed onto the fluorescent image in the uppermost panel. Arrows indicate the position of centrosomes.

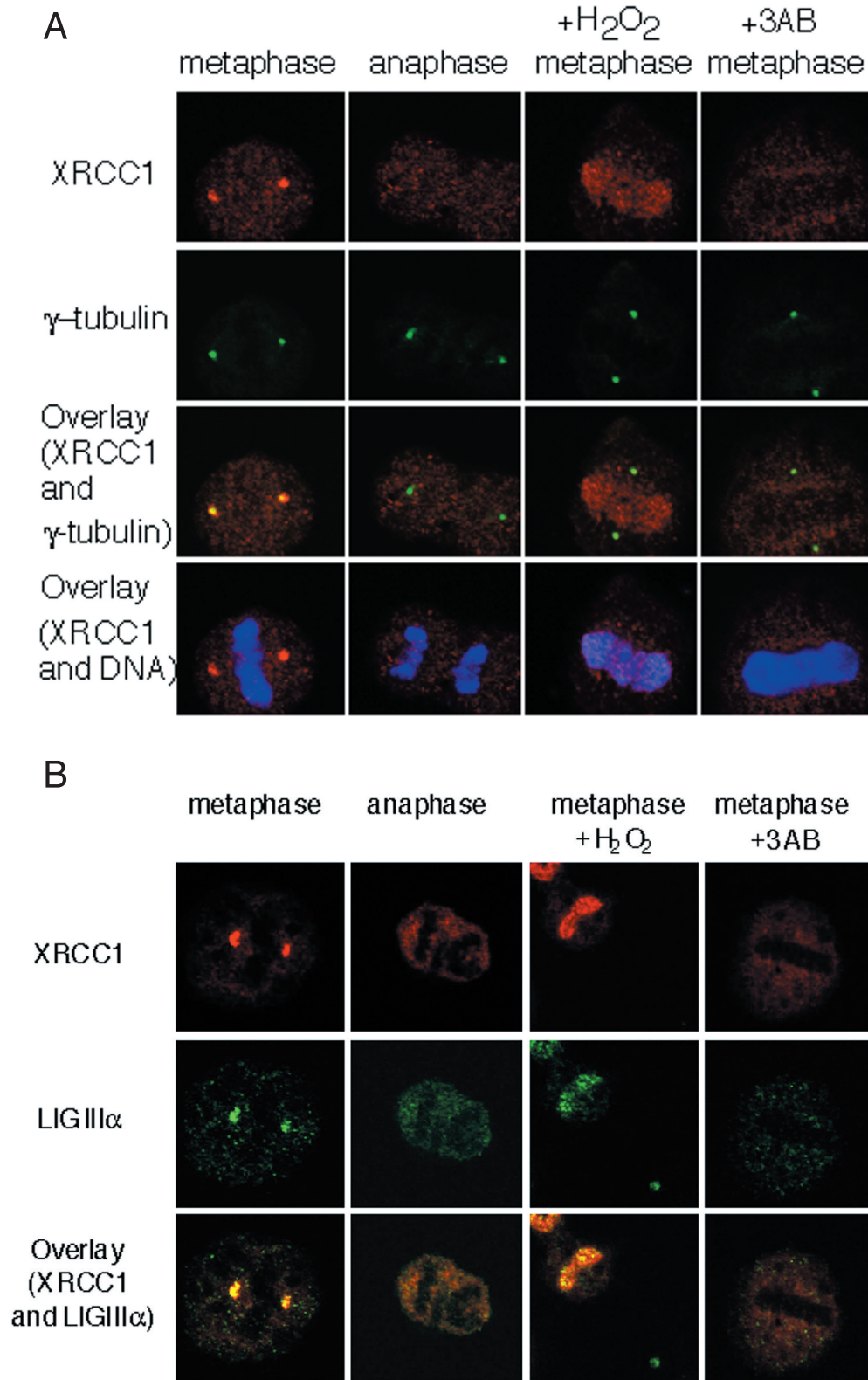
PAR glycohydrolase and, therefore, the amount of XRCC1 molecules is too low to be detected by western blotting analysis. Therefore, to confirm the centrosomal location of XRCC1, we transiently expressed a GFP-tagged XRCC1 in

HeLa cells. Indeed, in interphase cells, GFP-tagged XRCC1 was observed in the centrosomes (Figure 3B).

The association of a small fraction of XRCC1 with the centrosomes in interphase cells prompted us to examine the

behavior of XRCC1 during mitosis. Using TOPRO-3 to stain cellular DNA, we determined the distribution of XRCC1 and  $\gamma$ -tubulin (Figure 4A), XRCC1 and LIGIII $\alpha$  (Figure 4B), and XRCC1 and PAR (Figure 4C) at different stages of mitosis. As shown in these figures, in metaphase cells the majority of

XRCC1 co-localized with  $\gamma$ -tubulin in the centrosomes. XRCC1 was also detected at the periphery of the centrosomes in metaphase. XRCC1 accumulated at mitotic centrosome and its immediate vicinity in the cells from prophase to metaphase (Figures 5 and 4C, upper panels). However, the pericentriolar



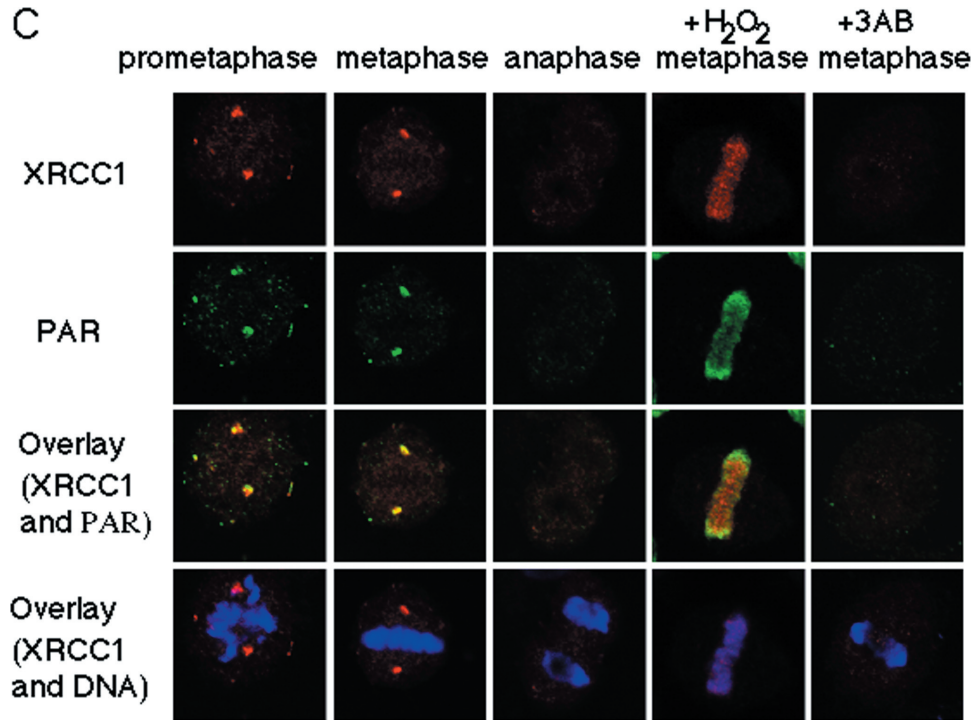


**Figure 4.** Co-localization of XRCC1 in the centrosomes of HeLa cells from different mitotic phases. (A) Double immunolabeling for XRCC1 and  $\gamma$ -tubulin. The cells were fixed with methanol:acetone and stained with anti-XRCC1 (red) and anti- $\gamma$ -tubulin (green) antibodies. Co-localization of the proteins appears yellow in the third row after overlay. DNA was stained with TOPRO-3 and superimposed onto the fluorescent images of the uppermost row (the bottom row). (B) Double immunolabeling for LIGIII $\alpha$  and XRCC1. The cells were fixed with paraformaldehyde and stained with anti-XRCC1 (red) and anti-LIGIII $\alpha$  (green) antibodies. Co-localization of the proteins appears yellow. (C) Double immunolabeling for PAR and XRCC1. The cells were fixed with methanol:acetone, and co-stained with anti-XRCC1 (red) and anti-PAR (green) antibodies. Panels in the first, the second and the third column are for untreated cells in prometaphase, metaphase and anaphase, respectively. Co-localization of the proteins appears yellow. DNA was stained with TOPRO-3 and superimposed onto the fluorescent images of the uppermost row (the bottom row).

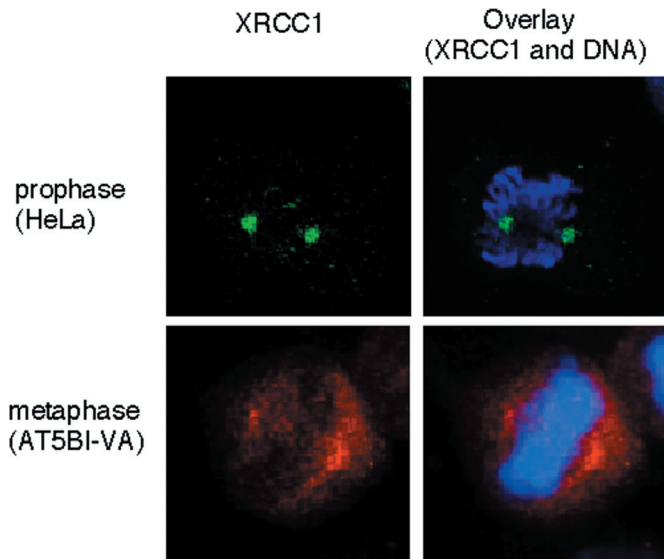


**Figure 5.** Distribution of XRCC1 in human cell lines. The upper left panel: fluorescent micrograph of HeLa cell in prophase by immunolabeling for XRCC1. The cells were fixed with paraformaldehyde, and stained with anti-XRCC1 monoclonal antibody. The lower left panel: fluorescent micrograph of AT5BI-VA cell in metaphase by immunolabeling for XRCC1. The cells were fixed with methanol:acetone, and stained with anti-XRCC1 antibody. The DNA was stained with TOPRO-3 and the corresponding images were superimposed onto the fluorescent images in the left columns and shown in the right columns.

localization of XRCC1 disappeared during anaphase (Figure 4A). A similar XRCC1 staining pattern was observed by using paraformaldehyde fixation (Figure 4B), and by using an XRCC1 monoclonal antibody (Figure 5) and in several human fibroblast cell lines including ATM-deficient (AT5BI-VA) cells (Figure 5). The staining pattern of LIGIII $\alpha$  detected with two different monoclonal antibodies was indistinguishable from that of XRCC1 (Figure 4B). Thus, we conclude that XRCC1 and LIGIII $\alpha$  are integral components of centrosomes, and that, during the early stages of mitosis, they also concentrate around the pericentriolar matrix.

**Localization of XRCC1 and LIGIII $\alpha$  to the centrosomes is dependent upon PAR synthesis**

To examine whether poly(ADP-ribosyl)ation is involved in the centrosomal localization of XRCC1, the cells were incubated with antibodies for PAR and XRCC1. PAR is reported to be present in the centrosomes in both interphase and mitosis (22). During mitosis, PAR co-localized with XRCC1 in the centrosomes and their immediate vicinity (Figure 4C). The change in the amount of PAR in the centrosomes and their immediate vicinity was completely correlated with that of XRCC1 (Figure 4C), suggesting the presence of yet unknown DNA damage-independent mechanisms of PARP activation and the recruitment of XRCC1 to the centrosomal region during mitosis. When cells were incubated for 1 h in

the presence of 3-AB (8 mM), a potent inhibitor of PARP, neither PAR nor XRCC1 was observed at or near centrosomes in metaphase cells (Figure 4A–C). Similarly, treatment with 3-AB abolished the localization of LIGIII $\alpha$  to the centrosomes of metaphase cells (Figure 4B). Moreover, in interphase cells, the centrosomal localization of XRCC1 was also prevented by 3-AB (data not shown). Together, these results show that the synthesis of PAR at or near the centrosomes is a prerequisite for the localization of both XRCC1 and LIGIII $\alpha$ .

#### **XRCC1 and LIGIII $\alpha$ translocate from centrosomal region to chromosomes after treatment of cells with H<sub>2</sub>O<sub>2</sub>**

Since PARP-1 is present in both centrosomes and chromosomes in mitotic cells (21), we examined whether during mitosis PARP is activated by DNA-damaging agents and whether this activation affects the localization of XRCC1 and LIGIII $\alpha$ . Following treatment of metaphase cells with H<sub>2</sub>O<sub>2</sub>, PAR was synthesized on the metaphase chromosomes (Figure 4C). In response to the PAR synthesis, both XRCC1 and LIGIII $\alpha$  were translocated from the centrosomes to the metaphase chromosomes (Figure 4A–C). Similar results were obtained by treating the cells with 100  $\mu$ M of DNA alkylating agent, MMS, for 10 min (data not shown). Thus, it appears that, as in interphase cells (19), the synthesis of PAR by PARP-1 at DNA strand breaks signals the recruitment of SSBs repair factors in mitotic cells. This suggests that DNA repair of SSBs occurs in the condensed chromatin of metaphase chromosomes.

#### **CONCLUSION**

Aneuploidy is a characteristic feature of cancer cells. The presence of an abnormally high number of centrosomes in human tumor cells including those lacking p53 suggests that dysregulation of centrosomes function may contribute to cancer formation (32,33). Recently, it has been reported that the PARP inhibitor 3-AB frequently causes centrosome hyperamplification (22). Here, we have shown that XRCC1 and LIGIII $\alpha$ , both of which interact with PARP-1, are present within the centrosomes in various stages of cell cycle. This effect is particularly evident in mitotic cells when the majority of these cellular proteins are localized at or near the centrosomes. Thus, it is possible that XRCC1 and LIGIII $\alpha$  are involved in the regulation of centrosome function. In this regard, it is worth noting that several single nucleotide polymorphisms associated with a variety of cancer types have been identified in the *XRCC1* gene [reviewed in (34)]. Alternatively, it is possible that the association of XRCC1 and LIGIII $\alpha$  with centrosomes in mitotic cells ensures the redistribution of these key DNA repair proteins to the daughter cells. Nonetheless, the DNA damage-dependent translocation of XRCC1 and LIGIII $\alpha$  from the centrosomes to the metaphase chromosomes provides evidence for DNA repair in the condensed chromatin of mitotic chromosomes. Further analysis of the roles of XRCC1 and LIGIII $\alpha$  in centrosome function and the repair of mitotic chromosomes will be important for understanding the causes of genomic instability in mitotic cells.

#### **ACKNOWLEDGEMENTS**

This work was supported in part by Grant-in-Aid for Scientific Research (nos 12143201 and 13480162) from the Ministry of Education, Science, Sports and Culture of Japan, by the Fund for ‘Studies on the Molecular Biological Basis for Low-Dose Radiation Effects’ from the Japan Atomic Energy Research Institute through a contract with the Nuclear Safety Research Association to A.Y. and by a grant (ES12512) to A.E.T. from the United States Public Health Service. Funding to pay the Open Access publication charges for this article was provided by Japan Society for the Promotion of Science.

#### **REFERENCES**

1. Thompson, L.H. and West, M.G. (2000) XRCC1 keeps DNA from getting stranded. *Mutat. Res.*, **459**, 1–18.
2. Dominguez, I., Daza, P., Natarajan, A.T. and Cortes, F. (1998) A high yield of translocations parallels the high yield of sister chromatid exchanges in the CHO mutant EM9. *Mutat. Res.*, **398**, 67–73.
3. Tebb, R.S., Flannery, M.L., Meneses, J.J., Hartmann, A., Tucker, J.D., Thompson, L.H., Cleaver, J.E. and Pedersen, R.A. (1999) Requirement for the *Xrcc1* DNA base excision repair gene during early mouse development. *Dev. Biol.*, **208**, 513–529.
4. Marsin, S., Vidal, A.E., Sossou, M., Menissier-de Murcia, J., Le Page, F., Boiteux, S., de Murcia, G. and Radicella, J.P. (2003) Role of XRCC1 in the coordination and stimulation of oxidative DNA damage repair initiated by the DNA glycosylase hOGG1. *J. Biol. Chem.*, **278**, 44068–44074.
5. Dantzer, F., de la Rubia, G., Menissier-de Murcia, J., Hostomsky, Z., de Murcia, G. and Schreiber, V. (2000) Base excision repair is impaired in mammalian cells lacking poly(ADP-ribose) polymerase-1. *Biochemistry*, **39**, 7559–7569.
6. Masson, M., Niedergang, C., Schreiber, V., Muller, S., Menissier-de Murcia, J. and de Murcia, G. (1998) XRCC1 is specifically associated with poly(ADP-ribose) polymerase and negatively regulates its activity following DNA damage. *Mol. Cell. Biol.*, **18**, 3563–3571.
7. Schreiber, V., Ame, J.C., Dolle, P., Schultz, I., Rinaldi, B., Fraulob, V., Menissier-de Murcia, J. and de Murcia, G. (2002) Poly(ADP-ribose) polymerase-2 (PARP-2) is required for efficient base excision DNA repair in association with PARP-1 and XRCC1. *J. Biol. Chem.*, **277**, 23028–23036.
8. Caldecott, K.W., Aoufouchi, S., Johnson, P. and Shall, S. (1996) XRCC1 polypeptide interacts with DNA polymerase beta and possibly poly(ADP-ribose) polymerase, and DNA ligase III is a novel molecular ‘nick-sensor’ *in vitro*. *Nucleic Acids Res.*, **24**, 4387–4394.
9. Kubota, Y., Nash, R.A., Klungland, A., Schar, P., Barnes, D.E. and Lindahl, T. (1996) Reconstitution of DNA base excision-repair with purified human proteins: interaction between DNA polymerase beta and the XRCC1 protein. *EMBO J.*, **15**, 6662–6670.
10. Vidal, A.E., Boiteux, S., Hickson, I.D. and Radicella, J.P. (2001) XRCC1 coordinates the initial and late stages of DNA abasic site repair through protein–protein interactions. *EMBO J.*, **20**, 6530–6539.
11. Whitehouse, C.J., Taylor, R.M., Thistlethwaite, A., Zhang, H., Karimi-Busheri, F., Lasko, D.D., Weinfeld, M. and Caldecott, K.W. (2001) XRCC1 stimulates human polynucleotide kinase activity at damaged DNA termini and accelerates DNA single-strand break repair. *Cell*, **104**, 107–117.
12. Caldecott, K.W., McKeown, C.K., Tucker, J.D., Ljungquist, S. and Thompson, L.H. (1994) An interaction between the mammalian DNA repair protein XRCC1 and DNA ligase III. *Mol. Cell. Biol.*, **14**, 68–76.
13. Caldecott, K.W., Tucker, J.D., Stanker, L.H. and Thompson, L.H. (1995) Characterization of the XRCC1-DNA ligase III complex *in vitro* and its absence from mutant hamster cells. *Nucleic Acids Res.*, **23**, 4836–4843.
14. Tomkinson, A.E., Chen, L.Z., Dong, Z., Leppard, J.B., Levin, D.S., Mackey, Z.B. and Motycka, T.A. (2001) Completion of base excision repair by mammalian DNA ligases. *Prog. Nucleic Acid Res. Mol. Biol.*, **68**, 151–164.
15. Taylor, R.M., Moore, D.J., Whitehouse, J., Johnson, P. and Caldecott, K.W. (2000) A cell cycle-specific requirement for the XRCC1 BRCT II domain during mammalian DNA strand break repair. *Mol. Cell. Biol.*, **20**, 735–740.

16. de Murcia,G. and Shall,S. (2000) *From DNA Damage and Stress Signaling to Cell Death*. Oxford University Press, Oxford, UK.
17. Burkle,A. (2001) Physiology and pathophysiology of poly(ADP-ribosyl)ation. *Bioessays*, **23**, 795–806.
18. Leppard,J.B., Dong,Z., Mackey,Z.B. and Tomkinson,A.E. (2003) Physical and functional interaction between DNA ligase III $\alpha$  and poly(ADP-Ribose) polymerase 1 in DNA single-strand break repair. *Mol. Cell. Biol.*, **23**, 5919–5927.
19. Okano,S., Lan,L., Caldecott,K.W., Mori,T. and Yasui,A. (2003) Spatial and temporal cellular responses to single-strand breaks in human cells. *Mol. Cell. Biol.*, **23**, 3974–3981.
20. Lan,L., Nakajima,S., Oohata,Y., Takao,M., Okano,S., Masutani,M., Wilson,S.H. and Yasui,A. (2004) *In situ* analysis of repair processes for oxidative DNA damage in mammalian cells. *Proc. Natl Acad. Sci. USA*, **101**, 13738–13743.
21. Kanai,M., Uchida,M., Hanai,S., Uematsu,N., Uchida,K. and Miwa,M. (2000) Poly(ADP-ribose) polymerase localizes to the centrosomes and chromosomes. *Biochem. Biophys. Res. Commun.*, **278**, 385–389.
22. Kanai,M., Tong,W.M., Sugihara,E., Wang,Z.Q., Fukasawa,K. and Miwa,M. (2003) Involvement of poly(ADP-Ribose) polymerase 1 and poly(ADP-Ribosyl)ation in regulation of centrosome function. *Mol. Cell. Biol.*, **23**, 2451–2462.
23. Augustin,A., Spenlehauer,C., Dumond,H., Menissier-De Murcia,J., Piel,M., Schmit,A.C., Apiou,F., Vonesch,J.L., Kock,M., Bornens,M. and de Murcia,G. (2003) PARP-3 localizes preferentially to the daughter centriole and interferes with the G1/S cell cycle progression. *J. Cell Sci.*, **116**, 1551–1562.
24. Smith,S. and de Lange,T. (1999) Cell cycle dependent localization of the telomeric PARP, tankyrase, to nuclear pore complexes and centrosomes. *J. Cell Sci.*, **112**, 3649–3656.
25. Ohashi,S., Kanai,M., Hanai,S., Uchiumi,F., Maruta,H., Tanuma,S. and Miwa,M. (2003) Subcellular localization of poly(ADP-ribose) glycohydrolase in mammalian cells. *Biochem. Biophys. Res. Commun.*, **307**, 915–921.
26. Okano,S., Kanno,S., Nakajima,S. and Yasui,A. (2000) Cellular responses and repair of single-strand breaks introduced by UV damage endonuclease in mammalian cells. *J. Biol. Chem.*, **275**, 32635–32641.
27. Sambrook,J., Fritsch,E.F. and Maniatis,T. (1989) *Molecular Cloning: A Laboratory Manual*, 2nd edn. Cold Spring Harbor Laboratory Press, Cold Spring Harbor, NY.
28. Taylor,R.M., Thistlethwaite,A. and Caldecott,K.W. (2002) Central role for the XRCC1 BRCT I domain in mammalian DNA single-strand break repair. *Mol. Cell. Biol.*, **22**, 2556–2563.
29. Mackey,Z.B., Ramos,W., Levin,D.S., Walter,C.A., McCarrey,J.R. and Tomkinson,A.E. (1997) An alternative splicing event which occurs in mouse pachytene spermatocytes generates a form of DNA ligase III with distinct biochemical properties that may function in meiotic recombination. *Mol. Cell. Biol.*, **17**, 989–998.
30. Nash,R.A., Caldecott,K.W., Barnes,D.E. and Lindahl,T. (1997) XRCC1 protein interacts with one of two distinct forms of DNA ligase III. *Biochemistry*, **36**, 5207–5211.
31. Jeng,R. and Stearns,T. (1999) Gamma-tubulin complexes: size does matter. *Trends Cell Biol.*, **9**, 339–342.
32. Fukasawa,K., Choi,T., Kuriyama,R., Rulong,S. and van de Woude,G.F. (1996) Abnormal centrosome amplification in the absence of p53. *Science*, **271**, 1744–1747.
33. Tarapore,P. and Fukasawa,F. (2000) p53 mutation and mitotic infidelity. *Cancer Invest.*, **18**, 148–155.
34. Ladiges,W., Wiley,J. and MacAuley,A. (2003) Polymorphisms in the DNA repair gene XRCC1 and age-related disease. *Mech. Ageing Dev.*, **124**, 27–32.